Brief Communication

MOLECULAR METABOLISM

Insulin controls food intake and energy balance via NPY neurons

Kim Loh [1,2,3,], Lei Zhang [1,2], Amanda Brandon [4,5], Qiaoping Wang [5], Denovan Begg [6], Yue Qi [1], Melissa Fu [1], Rishikesh Kulkarni [7], Jonathan Teo [6], Paul Baldock [7], Jens C. Brüning [8], Gregory Cooney [4,5], Greg Neely [5], Herbert Herzog [1,2,*]**

ABSTRACT

Objectives: Insulin signaling in the brain has been implicated in the control of satiety, glucose homeostasis and energy balance. However, insulin signaling is dispensable in energy homeostasis controlling AgRP or POMC neurons and it is unclear which other neurons regulate these effects. Here we describe an ancient insulin/NPY neuronal network that governs energy homeostasis across phyla.

Methods: To address the role of insulin action specifically in NPY neurons, we generated a variety of models by selectively removing insulin signaling in NPY neurons in flies and mice and testing the consequences on energy homeostasis.

Results: By specifically targeting the insulin receptor in both fly and mouse NPY expressing neurons, we found NPY-specific insulin signaling controls food intake and energy expenditure, and lack of insulin signaling in NPY neurons leads to increased energy stores and an obese phenotype. Additionally, the lack of insulin signaling in NPY neurons leads to a dysregulation of GH/IGF-1 axis and to altered insulin sensitivity.

Conclusions: Taken together, these results suggest that insulin actions in NPY neurons is critical for maintaining energy balance and an impairment of this pathway may be causally linked to the development of metabolic diseases.

Keywords Hypothalamus; NPY; Insulin; Obesity

1. INTRODUCTION

Insulin plays a critical role in the short-term as well as long-term control of glucose and energy homeostasis [1,2]. It fulfills this role by controlling both peripheral and central pathways to maintain glucose homeostasis and supply energy to various tissues and organs [1,2]. While the functions of insulin signaling in peripheral tissues have been studied extensively, its actions in the central nervous system are far less understood. Studies employing intracerebroventricular (i.c.v.) or intranasal administration of insulin or insulin mimetics have shown a significant effect of insulin signaling on decreasing appetite and body weight both in rodents and humans [3–6]. Further evidence comes from observations in models of reduced insulin or lack of insulin signaling in which a variety of central-mediated functions influencing energy homeostasis are altered, most prominently leading to hyperphagia and reduced energy metabolism [7,8].

Insulin receptors (IRs) are widely expressed in the brain and can be found prominently in hypothalamic nuclei like the arcuate nucleus (ARC) [9,10], which is known to be important in the control of feeding and energy homeostasis. The activity of the two main neuronal populations in this region, the anorexigenic pro-opiomelanocortin (POMC) and cocaine–amphetamine-regulated-transcript (CART) neurons as well as the orexigenic acting neuropeptide Y (NPY) and agouti-related peptide (AgRP) neurons are regulated by insulin signaling [11–13]. In the POMC/CART neurons the action of insulin is considered stimulatory to promote satiety while in the NPY/AgRP neurons the effect of insulin signaling is assumed to be mainly inhibitory to reduce appetite and increase energy expenditure [11–13].

The ability of insulin to regulate NPY expression is supported by several early studies showing that acute elevation of insulin levels by direct administration into the brain was able to reduce ARC NPY levels [12,13]. Consistent with this, NPY levels in the hypothalamus are strongly up-regulated in rodent models of insulin deficiency such as the streptozotocin (STZ) – diabetic rat, confirming an inhibitory tone by peripheral insulin [14]. Interestingly, the chronically elevated insulin levels that occur in obesity and insulin resistant states also lead to increased hypothalamic NPY levels, suggesting the development of resistance to the feedback effects of insulin on hypothalamic NPY [15,16]. Increased NPY levels contribute to the development of obesity in a two-fold manner, by increasing food intake as well as by reducing

[1]Neuroscience Division, Garvan Institute of Medical Research, St Vincent's Hospital, Sydney, 2010, Australia [2]Faculty of Medicine, UNSW, 2052, Australia [3]St. Vincent's Institute of Medical Research, Fitzroy, Victoria, 3065, Australia [4]Diabetes Division, Garvan Institute of Medical Research, St Vincent's Hospital, Sydney, 2010, Australia [5]Charles Perkins Center, University of Sydney, NSW, 2006, Australia [6]School of Psychology, UNSW, Sydney, NSW, 2052, Australia [7]Bone Biology Division, Garvan Institute of Medical Research, St Vincent's Hospital, Sydney, 2010, Australia [8]Max Planck Institute for Metabolism Research, Cologne, Germany

*Corresponding author. Neuroscience Division, Garvan Institute of Medical Research, St Vincent's Hospital, Sydney, 2010, Australia. E-mail: h.herzog@garvan.org.au (H. Herzog).

**Corresponding author. Neuroscience Division, Garvan Institute of Medical Research, St Vincent's Hospital, Sydney, 2010, Australia. E-mail: kloh@svi.edu.au (K. Loh).

Received March 8, 2017 • Revision received March 17, 2017 • Accepted March 30, 2017 • Available online 12 April 2017

http://dx.doi.org/10.1016/j.molmet.2017.03.013

energy expenditure mainly via down-regulation of brown adipose tissue (BAT) thermogenesis [16–18].

Additionally, central NPY also controls other peripheral systems including bone homeostasis and neuro-endocrine functions. Specifically by altering sympathetic tone, NPY controls the release of hormones including growth hormone releasing and thyrotropin releasing hormone [16]. Furthermore, action of NPY particularly in the paraventricular nucleus (PVN) of the hypothalamus, has also been shown to control parasympathetic outflow to the pancreas and, via this pathway, to stimulate insulin secretion [19]. On the other hand, NPY released from sympathetic neurons that innervate the pancreatic islets has the opposite effect, potently inhibiting insulin release [20]. Together, these findings suggest that there is a close regulatory loop by which NPY and insulin control expression and function of each other.

Interestingly, while global neuronal deletion of IRs leads to an obese phenotype [7], mice lacking IRs only in POMC or AgRP neurons exhibit unaltered food intake and energy balance [21]. Furthermore, selective deletion of the insulin receptor from Nkx2.1 and Sim1-positive neurons in the hypothalamus had no obvious effect on body weight or glucose homeostasis [22]. This indicates that other neuronal populations that do not contain POMC, AgRP, Nkx2.1, or Sim1 may be more critical for mediating the central regulation of feeding and energy homeostasis by insulin. One such candidate known to be a major player in this regulatory circuit is NPY [16]. Thus, to address the role of insulin action specifically in NPY neurons, we generated a variety of models by selectively removing insulin signaling in NPY neurons in flies and mice and testing the consequences on energy homeostasis.

2. RESULTS

2.1. NPY fulfills an evolutionary conserved role as an insulin signaling mediator in flies and mice

Deficiency of insulin signaling in AgRP or POMC neurons does not significantly influence feeding and energy homeostasis regulation in mice [21]. Fruit flies, *Drosophila melanogaster*, do not have AgRP or a melanocortin system; however, they do have an ancient form of NPY, called NPF, the ortholog of mammalian NPY [23]. In addition, flies also express insulin receptor (*InR*) on NPF neurons, making them an ideal model to study insulin action in the brain in the absence of melanocortin signaling [23,24]. To address the role of insulin signaling in NPF neurons, we used tissue-specific RNAi to generate flies in which insulin receptors (InR) are specifically knocked-down in NPF neurons (*NPF-Gal4>UAS-InR-IR*). Then, we analyzed several key parameters related to energy metabolism in these flies. Interestingly in *NPF-Gal4>UAS-InR* RNAi animals, food intake was significantly elevated (Figure 1A) whereas activity levels were unaltered (Figure 1B). This positive energy balance was confirmed by the increased storage of the excess energy in the form of glycogen (Figure 1C). Importantly, these stores were accessible and translated into enhanced survival during starvation in *NPF-Gal4>UAS-InR* knock-down flies (*$p < 0.05$, *NPF-Gal4/+* vs *NPF-Gal4>UAS-InR* RNAi) (Figure 1D). Taken together, these results demonstrate the crucial anorexigenic effect insulin signaling has on NPF neurons in the fly.

To investigate if this insulin/NPY exclusive pathway is also conserved in mammals, we generated NPY-neuron specific insulin-receptor (IR)-deficient mice by crossing $IR^{lox/lox}$ mice [7,21] with either mice expressing Cre-recombinase gene under the control of the mouse NPY promoter [25] ($IR^{lox/lox}$;$NPY^{Cre/+}$) or an inducible version of it [18] ($IR^{lox/lox}$;$NPY^{Cre/+,tm}$). Since the phenotype between $IR^{lox/lox}$ and $NPY^{Cre/+}$ mice did not show any obvious differences, $IR^{lox/lox}$ mice were used as controls for the germline model. Gene deletion in the inducible model was achieved by injecting mice with 3 doses of tamoxifen (75 mg/kg body weight/day for 3 days) at 8–10 week of age. Tamoxifen treated $IR^{lox/lox}$ mice ($IR^{lox/lox,tm}$) were used as controls. Successful IR deletion was confirmed in both models by PCR analysis of genomic DNA isolated from NPY expressing tissues, including the hypothalamus and olfactory bulb, while recombination was not detected in peripheral tissues that lack NPY expression, such as liver or muscle (Figure 1E–F).

To functionally prove that IRs were successfully deleted from NPY neurons, we injected $IR^{lox/lox}$;$NPY^{Cre/+}$ and $IR^{lox/lox}$ mice i.c.v. with either saline or insulin and stained for the activated form of the downstream insulin signaling molecule phosphorylated-Akt (p-Akt) in hypothalamic brain section of these mice. As shown in Figure 1G, insulin induced a strong increase of p-Akt positive neurons in the ARC in the $IR^{lox/lox}$, but this was significantly reduced in the $IR^{lox/lox}$;$NPY^{Cre/+}$ mice. Areas outside the hypothalamus did not show any obvious differences in activation of p-Akt between genotypes (data not shown), suggesting that NPY neurons in the hypothalamus are the critical population mediating insulin responses to energy homeostasis control. To further confirm that these are NPY neurons, we utilized our $IR^{lox/lox}$;$NPY^{Cre/+,tm}$ model which also co-expresses the fluorescence marker mCherry under the control of the NPY promoter. As expected, i.c.v. administration of insulin into the $IR^{lox/lox,tm}$ control mice produced a significant increase in p-Akt that showed extensive overlap with the mCherry expressing NPY neurons in the ARC (Figure 1H). In contrast, no overlap between mCherry and p-Akt was observed in tamoxifen induced $IR^{lox/lox}$;$NPY^{Cre/+,tm}$ mice (Figure 1H). Consistent with NPY being predominantly expressed in the hypothalamus, IR expression and insulin-induced Akt phosphorylation in NPY lacking tissues including muscle, WAT and liver were comparable between $IR^{lox/lox}$ and $IR^{lox/lox}$;$NPY^{Cre/+}$ mice (Supplemental Figure 1A–B).

One of the main consequences of insulin receptor activation in the hypothalamus is the up-regulation of *Pomc* mRNA and the corresponding down-regulation of *Npy* and *Agrp* expression [11,12,25]. Thus, we examined the effect of insulin on *Pomc*, *Agrp*, and *Npy* mRNA expression in $IR^{lox/lox}$ and $IR^{lox/lox}$;$NPY^{Cre/+}$ mice after an over-night fast. We found that $IR^{lox/lox}$ mice i.c.v. injected with insulin exhibit significantly enhanced hypothalamic *Pomc* mRNA levels and at the same time decreased *Agrp* and *Npy* expression as shown by quantitative real-time PCR (Figure 1I–K), consistent with previous reports [11,12,25]. In contrast, insulin injected into $IR^{lox/lox}$;$NPY^{Cre/+}$ mice was only able to increase *Pomc* expression but had no significant effect on *Agrp* and *Npy* mRNA levels (Figure 1I–K), further confirming the functionality of our model.

2.2. IR signaling in NPY neurons controls body weight and body composition

Unlike global neuronal insulin-receptor-deficient mice which exhibit impaired fertility [7], no difference in litter size, litter intervals, or gender ratio of pups (Supplemental Figure 2A) were noted between $IR^{lox/lox}$ and $IR^{lox/lox}$;$NPY^{Cre/+}$ mice, indicating that IR deficiency in NPY neurons does not impact upon reproductive fitness. Interestingly, however, body weights of 4-week-old germline $IR^{lox/lox}$;$NPY^{Cre/+}$ mice were significantly lower than those of $IR^{lox/lox}$ (Figure 2A), but this difference was reduced at 7–8 weeks of age. No overt difference in body weights or body length were noted between $IR^{+/+}$;$NPY^{Cre/+}$ and $IR^{lox/+}$;$NPY^{+/+}$ mice, consistent with the difference in body weight being due to IR deficiency in NPY neurons rather than influenced by the NPY-Cre transgene (Supplemental Figure 2B,C).

Furthermore, 4-week-old $IR^{lox/lox}$;$NPY^{Cre/+}$ mice showed significantly reduced lean body mass, coinciding with decreased body length, when

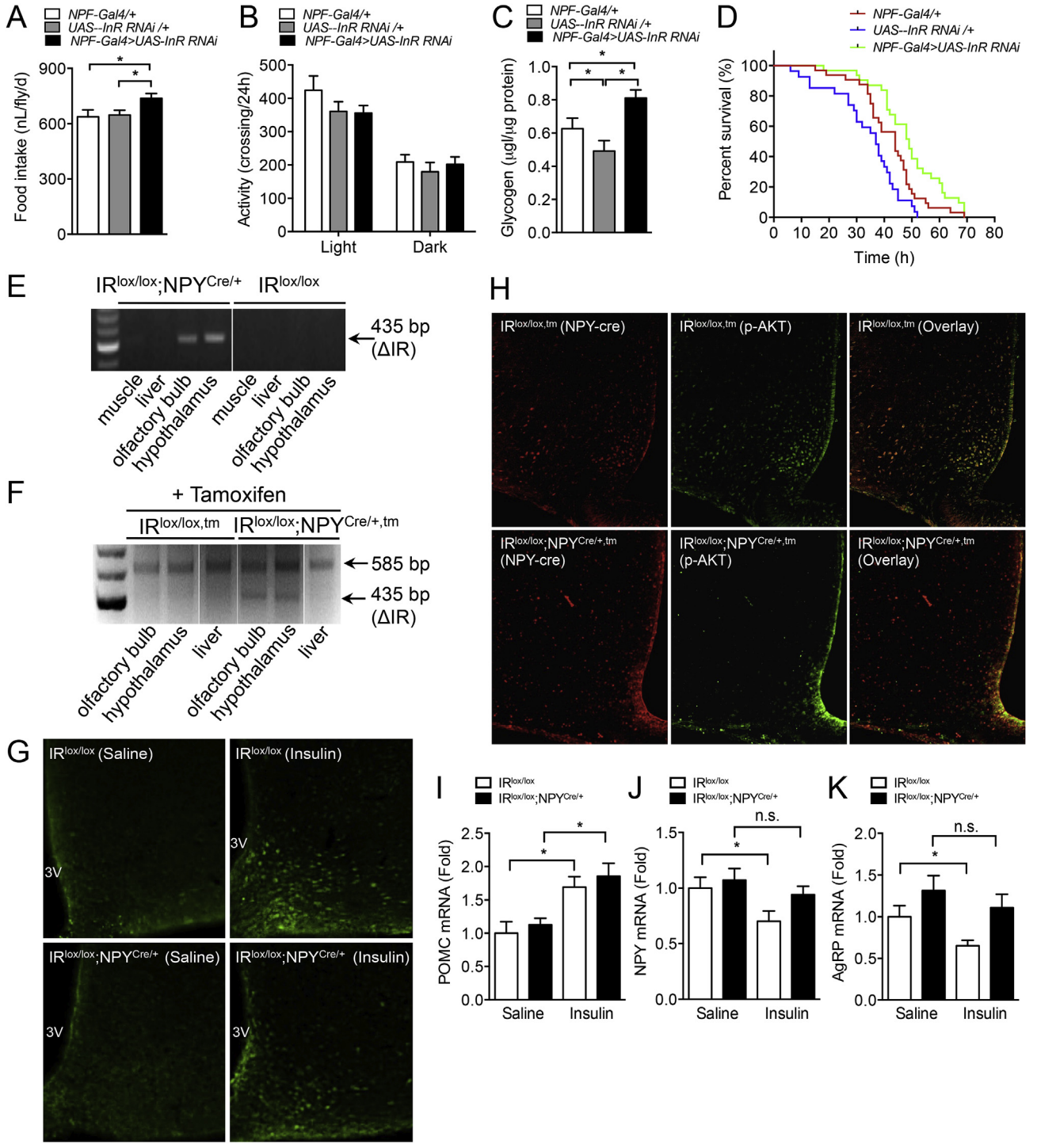

Figure 1: Increased food intake in NPF-specific insulin receptor knock-down flies. (A) Food intake in flies with *InR* RNAi knockdown in *NPF*+ neurons was significantly increased ($n \geq 9$, 5 animals per replicates). (B) Unaltered activity in flies with *InR* RNAi knockdown in *NPF*+ neurons ($n \geq 29$ animals). (C) Glycogen storage in flies with *InR* RNAi knockdown in *NPF*+ neurons was significantly increased ($n \geq 8$, 10 animals per replicates), one-way ANOVA with Welch's correction. (D) Flies with *InR* RNAi knockdown in *NPF*+ neurons survived longer under starvation ($n = 32$ animals). (E) Assessment of Cre-recombination at the level of genomic DNA in central and peripheral tissues of $IR^{lox/lox}$ and $IR^{lox/lox}$;$NPY^{Cre/+}$ mice. A 435 bp band confirms the rearrangement of the IR locus. (F) $IR^{lox/lox,tm}$ and $IR^{lox/lox}$;$NPY^{Cre/+,tm}$ mice were injected with 3 doses of tamoxifen (75 mg/kg body weight) and assessment of Cre-recombination at the level of genomic DNA in central and peripheral tissues. (G) $IR^{lox/lox}$ and $IR^{lox/lox}$;$NPY^{Cre/+}$ mice or (H) $IR^{lox/lox,tm}$ and $IR^{lox/lox}$;$NPY^{Cre/+,tm}$ were i.c.v. injected with either saline or insulin (2.5 mU in 2 µl), and PFA perfused brains were extracted and processed for immuno-histochemistry with antibodies to p-Akt. Representative photomicrographs showing p-Akt (Green), mCherry (Red), and colocalization (Yellow) in the ARC of the hypothalamus. (I–K) $IR^{lox/lox}$ and $IR^{lox/lox}$;$NPY^{Cre/+}$ mice were fasted overnight and i.c.v. injected with saline or insulin (10 mU in 2 µl, 2 h), RNA was isolated from hypothalami and expression of *Pomc*, *Agrp*, and *Npy* mRNA were determined using quantitative RT-PCR. *Rpl19* was used as control. (E–K, $n = 3$–5 per group). Data are means ± SEM. *$p < 0.05$.

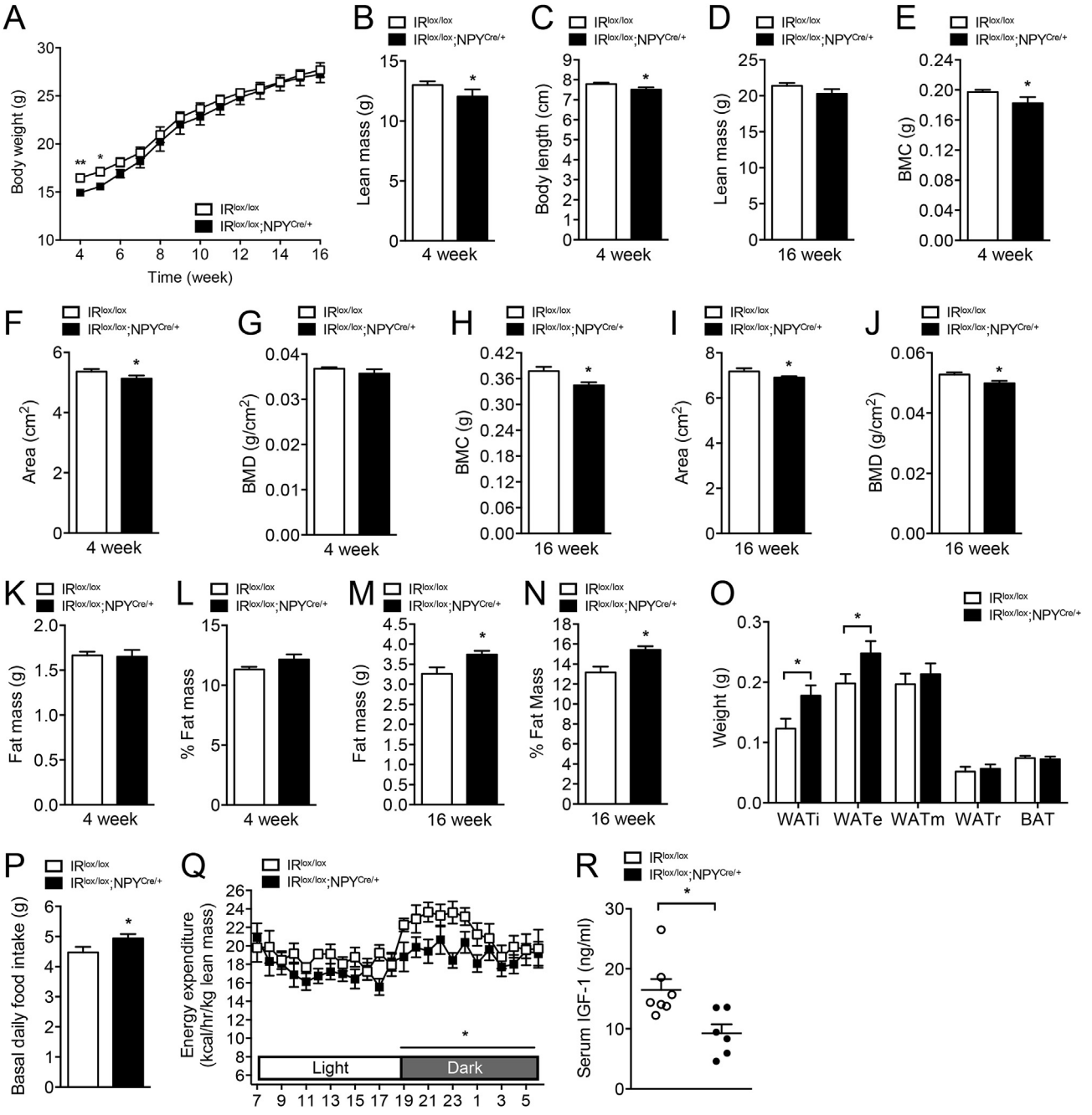

Figure 2: Altered food intake and energy homeostasis in NPY-neuron specific IR-deficient mice. (A) Body weight curve of $IR^{lox/lox}$ and $IR^{lox/lox}$;$NPY^{Cre/+}$ mice. (B–D) Body length and whole body lean mass determined by DXA. (E–G) Bone mineral content (BMC), bone area, and bone mineral density (BMD) determined in 4-week-old $IR^{lox/lox}$ and $IR^{lox/lox}$;$NPY^{Cre/+}$ mice and (H–J) 16-week-old $IR^{lox/lox}$ and $IR^{lox/lox}$;$NPY^{Cre/+}$ mice. (K, L) Body fat mass determined by DXA scan and normalized to body weight in 4-week-old $IR^{lox/lox}$ and $IR^{lox/lox}$;$NPY^{Cre/+}$ mice and (M, N) 16-week-old $IR^{lox/lox}$ and $IR^{lox/lox}$;$NPY^{Cre/+}$ mice. (O) Absolute weights of adipose tissues from inguinal (WATi), epididymal (WATe), mesenteric (WATm), and retroperitoneal (WATr) depots and intrascapular brown adipose tissue (BAT) measured in 16-week-old chow fed $IR^{lox/lox}$ and $IR^{lox/lox}$;$NPY^{Cre/+}$ mice. (P) Basal daily food intake assessed in 16-week-old $IR^{lox/lox}$ and $IR^{lox/lox}$;$NPY^{Cre/+}$ mice. (Q) Light and dark cycle energy expenditure (normalized to total lean mass) determined in metabolic chambers in 16-week-old $IR^{lox/lox}$ and $IR^{lox/lox}$;$NPY^{Cre/+}$ mice. (R) Serum IGF-1 levels determined in 16-week-old $IR^{lox/lox}$ and $IR^{lox/lox}$;$NPY^{Cre/+}$ mice. Data are means ± SEM of 7–10 mice per group. *$p < 0.05$, **$p < 0.01$.

analyzed by whole body dual energy X-ray absorptiometry (DXA) (Figure 2B, C). However, this difference in lean mass diminished over time and was not statistically significant in older mice (Figure 2D). Consistent with the known involvement of hypothalamic NPY neurons in the central control of bone homeostasis [27], lack of IR signaling in these neurons results in a reduction in bone mineral density, bone area, and bone mineral content (Figure 2E–G). Contrary to the other parameters investigated above, this reduced bone mass does not recover over time (Figure 2H–J).

More importantly, body fat mass was increased as a result of IR deficiency in NPY neurons. Although no difference in fat mass is noted in 4-week-old $IR^{lox/lox}$;$NPY^{Cre/+}$ mice (Figure 2K, L), over time, the lack of IR

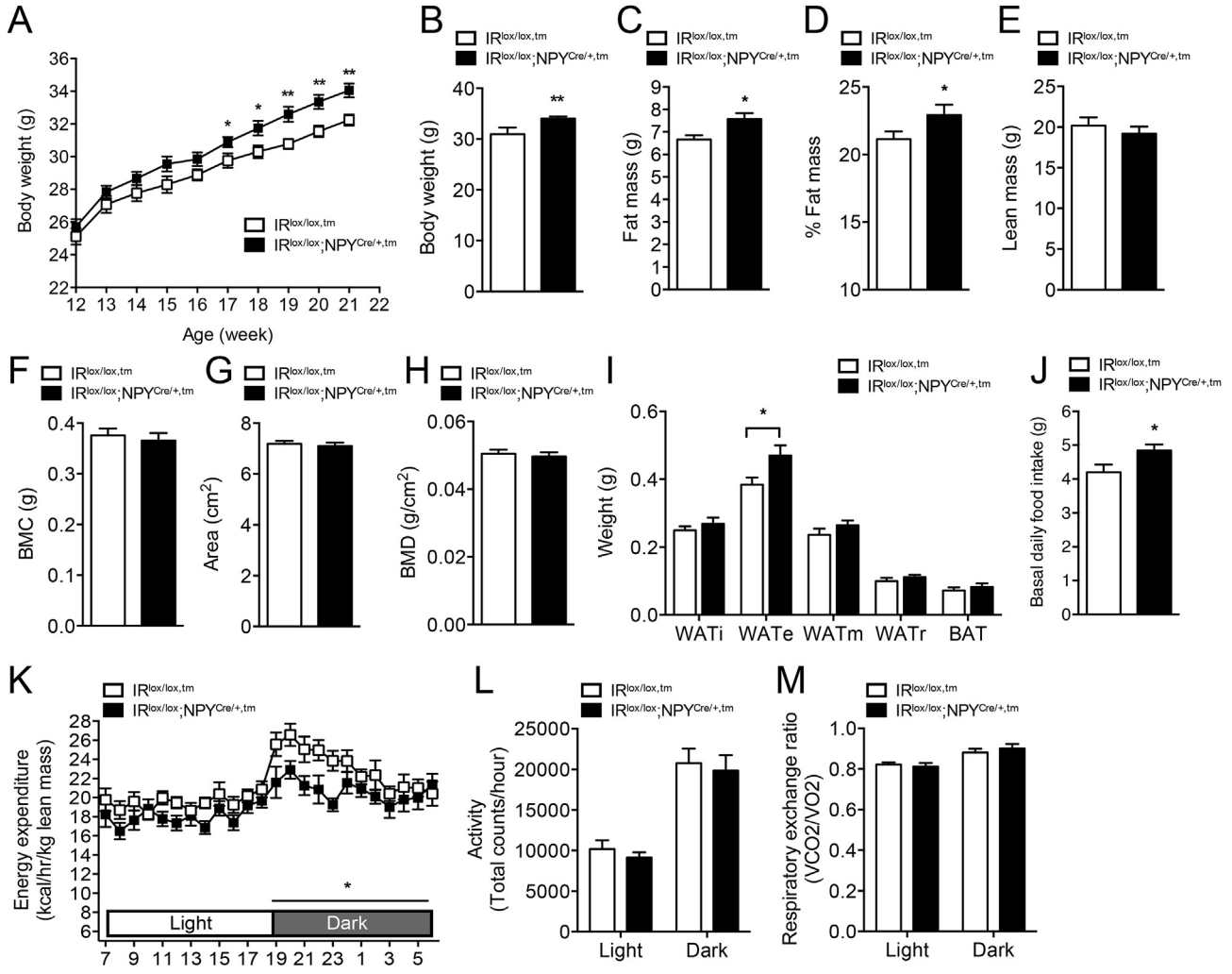

Figure 3: Impaired energy balance in adult onset deleted NPY-neuron specific IR-deficient mice. (A) Body weight curve of $IR^{lox/lox,tm}$ and $IR^{lox/lox}$;$NPY^{Cre/+,tm}$ mice measured on a weekly basis starting from the time of tamoxifen injection. (B) Body weights were measured after 10 weeks post-tamoxifen injection. (C–E) Body composition (lean and fat mass) determined by DXA scan and normalized to body weight in $IR^{lox/lox,tm}$ and $IR^{lox/lox}$;$NPY^{Cre/+,m}$ mice. (F–H) Bone mineral content (BMC), bone area, and bone mineral density (BMD) determined in $IR^{lox/lox,tm}$ and $IR^{lox/lox}$;$NPY^{Cre/+,tm}$ mice. (I) Absolute weights of adipose tissues from inguinal (WATi), epididymal (WATe), mesenteric (WATm), and retroperitoneal (WATr) depots and intrascapular brown adipose tissue (BAT) measured from $IR^{lox/lox,tm}$ and $IR^{lox/lox}$;$NPY^{Cre/+,tm}$ mice. (J) Basal daily food intake assessed in $IR^{lox/lox,tm}$ and $IR^{lox/lox}$;$NPY^{Cre/+,tm}$ mice. (K–M) Light and dark cycle energy expenditure (normalized to total lean mass), ambulatory activity, and respiratory exchange ratio determined in metabolic chambers in $IR^{lox/lox,tm}$ and $IR^{lox/lox}$;$NPY^{Cre/+,tm}$ mice. Data are means ± SEM of 7–10 mice per group. *p < 0.05, **p < 0.01.

signaling led to significantly increased fat mass, both in absolute terms as well as expressed as percent of total body weight (Figure 2M, N). Consistent with this, the weights of individual dissected white adipose tissues depots, including the inguinal (i) and epididymal (e), were significantly elevated in 16-week-old $IR^{lox/lox}$;$NPY^{Cre/+}$ mice (Figure 2O). Interestingly, mesenteric and retroperitoneal fat mass depots are not different, suggesting that the lack of insulin signaling in NPY neurons leads to a selective increase of fat accumulation in specific depots.

2.3. Impaired energy homeostasis in NPY-neuron specific IR-deficient mice

In order to determine if one or both sides of the energy balance equation had been altered to drive the increase in body weight and fat mass in $IR^{lox/lox}$;$NPY^{Cre/+}$ mice, we next investigated food consumption and energy expenditure. In line with NPY's role as a potent appetite stimulant, spontaneous food intake in $IR^{lox/lox}$;$NPY^{Cre/+}$ mice was significantly increased (Figure 2P). On the other hand, fasting induced food intake was not different between the genotypes, most likely due to the maximal hypothalamic NPY response being reached under fasting condition (Supplemental Figure 2D). To test the effects of IR deficiency in NPY neurons on energy expenditure, indirect calorimetric was performed on $IR^{lox/lox}$;$NPY^{Cre/+}$ mice, which revealed a significant decrease in energy expenditure compared to $IR^{lox/lox}$ mice (Figure 2Q). By contrast, ambulatory activity and respiratory exchange ratio (RER) (Supplemental Figure 2E, F) were similar between $IR^{lox/lox}$;$NPY^{Cre/+}$ and $IR^{lox/lox}$ mice. Taken together, these results indicate that both increased food intake and reduced energy expenditure contribute to the increased body weight gain and late-onset adiposity in $IR^{lox/lox}$;$NPY^{Cre/+}$ mice, consistent with the classical functions of elevated NPY levels in the hypothalamus.

2.4. IR deficiency in NPY neurons leads to perturbation of the GH/IGF-1 axis

In addition to the major role NPY plays in controlling energy balance, NPY has also been shown to influence the neuro-endocrine axis [16].

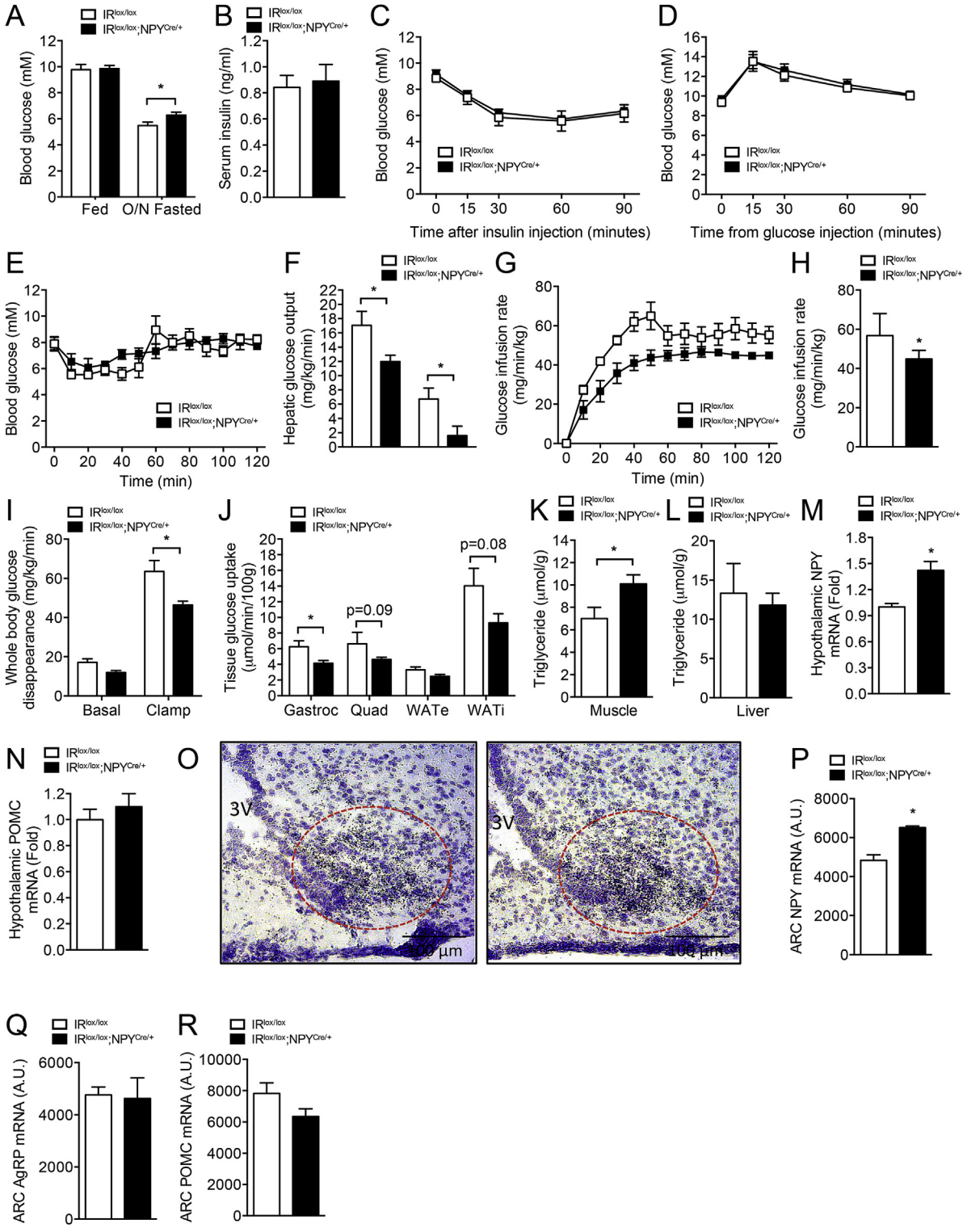

Figure 4: Reduced glucose uptake and enhanced hypothalamic NPY expression in $IR^{lox/lox}$;$NPY^{Cre/+}$ mice. (A) Fed and overnight (O/N) fasted blood glucose levels and (B) serum insulin levels determined in 16-week-old $IR^{lox/lox}$ and $IR^{lox/lox}$;$NPY^{Cre/+}$ mice. (C–D) Blood glucose levels in $IR^{lox/lox}$ and $IR^{lox/lox}$;$NPY^{Cre/+}$ mice undergoing insulin tolerance and glucose tolerance tests, respectively. (A–D, n = 7–10 per group). Hyperinsulinemic-euglycemic clamp studies in $IR^{lox/lox}$ and $IR^{lox/lox}$;$NPY^{Cre/+}$ mice. (E) Blood glucose and (F) hepatic glucose output during basal and insulin stimulated conditions. (G–H) Glucose infusion rate during the clamp. (I) Whole body glucose disappearance and glucose uptake into (J) gastrocnemius (gastroc) and quadriceps (quad) muscles and epididymal (WATe) and inguinal (WATi) fat pads. (K–L) Muscle and liver triglyceride levels in $IR^{lox/lox}$ and $IR^{lox/lox}$;$NPY^{Cre/+}$ mice. (E–L, n = 5–7 per group). (M–N) Hypothalamic *Npy* and *Pomc* expression in $IR^{lox/lox}$ and $IR^{lox/lox}$;$NPY^{Cre/+}$ mice determined by qRTPCR. (O–R) Brain slices from $IR^{lox/lox}$ and $IR^{lox/lox}$;$NPY^{Cre/+}$ showing *in situ* hybridization of *Npy*, *Agrp*, and *Pomc*. Representative photographs showing expression of *Npy* mRNA in the ARC of $IR^{lox/lox}$ and $IR^{lox/lox}$;$NPY^{Cre/+}$ mice (M–R, n = 4–5 per group). Data are expressed as mean ± SEM. *p < 0.05.

Importantly, studies from Peirroz et al. have shown that chronic administration of NPY (signaling a negative energy balance) abolished pulsatile secretion of growth hormone (GH), which, in turn, leads to decreases in circulating insulin-growth-factor-1 (IGF-1) levels [28]. By contrast, administration of an antibody to NPY causes a significant increase in circulating GH levels [29]. Given that perturbation in the GH/IGF-1 axis strongly influences muscle mass [30], we hypothesized that the GH/IGF-1 axis is altered in $IR^{lox/lox}$;$NPY^{Cre/+}$ mice and this may contribute to the reduced lean mass (Figure 1C). Indeed, $IR^{lox/lox}$;$NPY^{Cre/+}$ mice showed significantly reduced serum IGF-1 levels (Figure 2R) and this, together with the observed effects on appetite and energy expenditure, may be the driving forces that leads to the late onset obesity phenotype in these mice.

2.5. Adult onset deletion of IR in NPY neurons replicates the germline phenotype

Since germline deletion can cause developmental compensation effects, we also tested the consequences of selective ablation of insulin signaling in NPY neurons in an adult onset model (Figure 1F). For this, 8–10-week-old, $IR^{lox/lox,tm}$ and $IR^{lox/lox}$;$NPY^{Cre/+,tm}$ mice were injected with tamoxifen to induce the gene deletion and body weight and other metabolic parameters were monitored over the next 12 weeks. Body weights between $IR^{lox/lox,tm}$ and $IR^{lox/lox}$;$NPY^{Cre/+,tm}$ mice were not significantly different at the time of induction of gene deletion (Figure 3A). However, consistent with germline $IR^{lox/lox}$;$NPY^{Cre/+}$ mice, $IR^{lox/lox}$;$NPY^{Cre/+,tm}$ mice exhibited significantly increased weigh gain after induction of IR gene deletion compared to $IR^{lox/lox,tm}$ mice (Figure 3A, B), which was associated with significantly increased fat mass (absolute as well as percent of body weight) (Figure 3C, D). In contrast to germline $IR^{lox/lox}$/$NPY^{cre/+}$ mice, however, adult onset induced $IR^{lox/lox}$;$NPY^{Cre/+,tm}$ mice did not exhibit any differences in lean mass (Figure 3E) or bone mass (Figure 3F–H) when compared to controls, suggesting that alterations in these parameters might be dependent on IR signaling during early development. Consistent with the observed increased whole body adiposity, individual dissected fat depots also revealed a significant increase in WATe in $IR^{lox/lox}$;$NPY^{Cre/+,tm}$ mice (Figure 3I). The cause for the increased adiposity in these mice, like in the germline $IR^{lox/lox}$;$NPY^{Cre/+}$ mice, is most likely due to the significant increase in food intake and the coinciding reduction in energy expenditure (Figure 3J, K). Consistent with the germline deletion model, physical activity and RER were again unaltered by the adult onset deletion of the IR in NPY neurons (Figure 3L, M). Taken together, the consistency of the germline and adult onset $IR^{lox/lox}$;$NPY^{Cre/+}$ phenotypes demonstrates that the altered feeding behavior and energy expenditure are the direct consequence of lack of IR signaling in NPY neurons rather than the results of developmental effects.

2.6. Lack of IR signaling in NPY neurons does not exacerbate high-fat diet-induced obesity

Elevated insulin levels are common under insulin resistance or positive energy balance conditions, which can be introduced by high caloric, high-fat diets. To examine the importance of IR signaling in NPY neurons in the development of obesity, we next assessed the impact of IR deficiency in $IR^{lox/lox}$;$NPY^{Cre/+}$ mice on a high-fat diet (HFD). Interestingly, in contrast to the observed differences in body weight gain seen in chow fed $IR^{lox/lox}$;$NPY^{Cre/+}$ mice, no significant differences were noted between $IR^{lox/lox}$;$NPY^{Cre/+}$ and $IR^{lox/lox}$ mice fed a high-fat diet for 8 weeks (Supplemental Figure 3A), and consistent with this, no differences in whole body fat mass (Supplemental Figure 3B, C) nor individual dissected fat depots (Supplemental Figure 3D) was observed. However, HFD-fed $IR^{lox/lox}$;$NPY^{Cre/+}$ mice displayed a trend to decreased lean body mass (Supplemental Figure 3E) and showed a significant reduction in bone mineral content and bone mineral density as determined by whole body DXA scans (Supplemental Figure 3G, H) consistent with the early onset of these differences in the chow $IR^{lox/lox}$;$NPY^{Cre/+}$ mice. Interestingly, while there were significant differences in energy expenditure and food intake in $IR^{lox/lox}$;$NPY^{Cre/+}$ mice fed a chow diet, none of these effects were seen in high-fat diet fed $IR^{lox/lox}$;$NPY^{Cre/+}$ mice (Supplemental Figure 3I–L).

2.7. Impaired glucose homeostasis in NPY-neuron specific IR-deficient mice

Central NPY pathways have been implicated in the control of glucose homeostasis and it has been shown that i.c.v. administration of NPY abolishes insulin's ability to suppress hepatic glucose production [31,32]. Therefore, we next investigated whether specific IR deletion in NPY neurons also causes similar disruptions to glucose homeostasis. Basal non-fasted blood glucose levels were comparable between $IR^{lox/lox}$;$NPY^{Cre/+}$ and $IR^{lox/lox}$ mice (Figure 4A). Interestingly, however, $IR^{lox/lox}$;$NPY^{Cre/+}$ mice exhibited significantly higher fasting blood glucose levels (Figure 4A). Consistent with unaltered blood glucose levels, serum insulin concentrations in the fed state were indistinguishable between $IR^{lox/lox}$;$NPY^{Cre/+}$ and $IR^{lox/lox}$ mice (Figure 4B). Despite the higher fasting blood glucose levels, glucose clearance and insulin responsiveness, as determined by glucose and insulin tolerance tests, respectively, were similar in $IR^{lox/lox}$;$NPY^{Cre/+}$ and $IR^{lox/lox}$ mice (Figure 4C, D). However, it is possible that the elevated fasting glucose levels in the $IR^{lox/lox}$;$NPY^{Cre/+}$ mice could be a consequence of altered hepatic glucose production. Therefore, to assess this and the contribution that individual tissues make in the regulation of glucose homeostasis more comprehensively, hyperinsulinemic-euglycemic clamps were performed on $IR^{lox/lox}$;$NPY^{Cre/+}$ and $IR^{lox/lox}$ mice.

In the basal state, there was no difference in blood glucose, insulin, or NEFA levels (Figure 4E, Supplemental Figure 4A), but hepatic glucose output (HGO) was lower in the $IR^{lox/lox}$;$NPY^{Cre/+}$ than $IR^{lox/lox}$ animals (Figure 4F). Under clamped conditions, the $IR^{lox/lox}$;$NPY^{Cre/+}$ animals exhibited a lower glucose infusion rate (GIR) (Figure 4G, H) than the $IR^{lox/lox}$ mice, coinciding with significantly reduced whole body glucose uptake (Figure 4I), indicating that the $IR^{lox/lox}$;$NPY^{Cre/+}$ animals were insulin resistant. Interestingly, the liver was not resistant to the effects of insulin with HGO being lower in the clamped state (Figure 4F) and the percentage suppression of HGO by insulin during the clamp was not different from that of $IR^{lox/lox}$ mice (data not shown). The whole-body insulin resistance was due to a decrease in peripheral glucose uptake. More specifically, glucose uptake into the gastrocnemius muscle was significantly reduced in the $IR^{lox/lox}$;$NPY^{Cre/+}$ animals, also with a strong tendency to be lower in the quadriceps muscle ($p = 0.09$) and epididymal and subcutaneous fat pads ($p = 0.08$; Figure 4J). While no differences in liver triglyceride content was noted, the decrease in glucose uptake into the muscles in the $IR^{lox/lox}$;$NPY^{Cre/+}$ animals was accompanied by an increase in the triglyceride content, which is often a correlate of insulin resistance in muscle (Figure 4K, L).

2.8. Enhanced hypothalamic NPY expression in $IR^{lox/lox}$;$NPY^{Cre/+}$ mice

To investigate the underlying mechanism that leads to the altered energy metabolism and the discrepancies between chow and HFD phenotypes, we next examined the expression of *Npy* mRNA in the hypothalamus of mice fed *ad libitum*. Consistent with the results shown in Figure 1J, in which insulin administration leads to a suppression of *Npy* expression, lack of insulin signaling leads to significant up-regulation of hypothalamic *Npy* expression in $IR^{lox/lox}$;$NPY^{Cre/+}$

mice, whereas hypothalamic *Pomc* mRNA expression was unaltered (Figure 4M, N). It is interesting to note that the up-regulation of *Npy* expression in $IR^{lox/lox}$;$NPY^{Cre/+}$ versus $IR^{lox/lox}$ mice under fed condition (Figure 4M) was absent under fasting condition (Figure 1J), which is likely due to masking effects of other factors that act during energy deficit to up-regulate NPY. On the other hand, the differences in *Npy* mRNA levels between $IR^{lox/lox}$;$NPY^{Cre/+}$ and $IR^{lox/lox}$ mice were no longer obvious after mice were fed a high-fat diet, and there was also no difference in expression of *Pomc* mRNA between genotypes (Supplemental Figure 4B, C), consistent with no significant differences in energy balance and appetite being noted in HFD fed $IR^{lox/lox}$;$NPY^{Cre/+}$ mice.

Having established that impaired insulin signaling leads to enhanced hypothalamic *Npy* expression in $IR^{lox/lox}$;$NPY^{Cre/+}$ mice, we next focused on identifying the specific nuclei in the hypothalamus that mediates insulin-NPY in the regulation of energy balance and appetite. To examine this, we determined *Npy* mRNA levels in the hypothalamic sections of $IR^{lox/lox}$;$NPY^{Cre/+}$ and $IR^{lox/lox}$ mice fed *ad libitum* by *in situ* hybridization, and we found that *Npy*, but not *Agrp*, expression was significantly elevated in the ARC of the hypothalamus (Figure 4O–Q). Importantly, the lack of change in *Pomc* mRNA levels is consistent with IR signaling being less important in these neurons (Figure 4R), confirming that defective IR signaling in NPY neurons is the main driver that leads the development of an obesity phenotype in $IR^{lox/lox}$;$NPY^{Cre/+}$ mice.

3. DISCUSSION

While previous studies have indicated a role of insulin signaling in the brain, the particular neuronal population mediating these effects was unknown. In this study, we now demonstrate that NPY-expressing neurons are critical in mediating the central actions of insulin in the regulation of appetite and energy homeostasis, since lack of IR signaling in NPY neurons leads to increased body weight and adiposity attributable to significantly increased food intake and reduced energy expenditure. The absence of IR signaling in NPY neurons also leads to a significant up-regulation of hypothalamic *Npy* expression, which is consistent with the observed increase in appetite and reduced energy expenditure as well as reduced bone mass [27]. Interestingly, $IR^{lox/lox}$;$NPY^{Cre/+}$ mice also exhibited reduced lean mass that is accompanied by significant reduction in circulating IGF-1 levels. Importantly, the phenotype of the germline $IR^{lox/lox}$;$NPY^{Cre/+}$ mice, with the exception of effects on bone mass, was replicated in the adult onset $IR^{lox/lox}$;$NPY^{Cre/+,tm}$ model, confirming the critical contribution of insulin signaling in NPY neurons as the primary cause of the observed effects. The reduction in bone mass specifically in the early onset deletion model, which does not recover over time, highlights the critical influence that NPY signaling has on the central control of bone homeostasis and that imbalances in this system during early development can have severe consequences later in life. Together, results from this study provide conclusive evidence that IR signaling in NPY-expressing neurons is a key contributor for insulin's action in the regulation of feeding and energy expenditure.

These findings are also consistent with the hyperphagia found in mice with global neuronal specific inactivation of IR [7], in mice with IR selectively downregulated in the ARC or PVN of the hypothalamus [8], and in studies using pharmacological IR signaling inhibitors [33]. Interestingly, studies that investigated the metabolic phenotypes of mice lacking the IR in POMC, AgRP, Nkx2.1, or Sim1 neurons did not show any significant alteration in energy homeostasis parameters due to this manipulation. In light of our results, the lack of effects in AgRP neuron-specific insulin receptor deficient mice is somewhat surprising, since it is assumed that AgRP neurons are 100% NPY co-expressing. However, this notion that most, if not all, ARC NPY neurons are also AgRP positive has been challenged, and there is increasing evidence that a considerable number of NPY neurons in the ARC do not contain AgRP [17,34]. Importantly, a recent comprehensive mapping of ARC neurons clustering them into different groups has identified a subset of NPY neurons that is devoid of AgRP but instead co-expresses neurotensin [35]. This highlights the potential that this NPY neuron subpopulation that lacks AgRP in the ARC may have a more critical function in mediating insulin responses related to feeding and energy expenditure to the brain. Therefore, selective deletion of IRs in AgRP neurons might only reveal parts of the known insulin-controlled NPY activities and might explain the lack of a hyperphagic phenotype in models with AgRP neuron-restricted inactivation of IR [21]. Our results also suggest that the specific population of NPY neurons that mediate these effects of insulin on feeding and energy expenditure seem to be distinct and less likely to be those neurons that co-express AgRP. In addition, the regulation of food intake by insulin in non-hypothalamic NPY neurons may also be a key contributing factor to the overall phenotypes. This was supported by previous studies in which insulin administration reduced NPY expression in amygdala, leading to a significant reduction in food intake [36,37]. While other contributions from NPY/AgRP co-expressing neurons to the overall control of energy homeostasis cannot be completely excluded, this neuronal population does not seem to be critical for mediating insulin actions in the regulation of feeding and energy expenditure.

Interestingly, while there is a clear difference in the obesity phenotype observed in chow fed $IR^{lox/lox}$;$NPY^{Cre/+}$ compared to control mice, under conditions of a prolonged positive energy balance induced by high-fat feeding, the genotype differences are no longer obvious. One explanation for this could be the induction of central insulin resistance [15,38]. In addition, it could also suggest that other factors might be able to compensate for the lack of insulin control on feeding and energy expenditure. For instance, it has been shown that NPY-induced appetite stimulation can be influenced in response to circadian and palatability cues [39]. Moreover, considering the increased fat mass as a consequence of chronic high-fat feeding the elevated serum leptin levels under these conditions may compensate for the lack of insulin control of hypothalamic NPY neurons and mask insulin deficiency in this context.

Central NPY is known to influence peripheral insulin release indirectly via parasympathetic pathways with increased central NPY stimulating insulin release from pancreatic beta-cells, followed by insulin action on hypothalamic NPY neurons to reduce NPY levels. This loop of reciprocal control between these two factors seems to be critical for maintaining a balanced energy homeostasis. Imbalances in this feedback loop as generated by our models confirm this critical function but also highlight the involvement of central NPY in other aspects of peripheral insulin function including the development of insulin resistance due to decreased skeletal muscle glucose uptake as shown in our clamp study. One likely explanation for the decreased insulin action in muscle is that hyperphagia and lipid accumulation observed in adipose tissue and muscle when IR are deleted from NPY neurons generates insulin resistance via some combination of substrate competition and decreased insulin signaling [40]. On the other hand, considering the inhibitory nature of insulin action on NPY neuronal activity, this finding is consistent with results from a recent report showing that insulin resistance develops upon acute activation of NPY positive neurons in the ARC [41]. Our results are in contrast to studies that show increased NPY expression and food intake in response to neuroglucopenia induced by insulin administration [42]. However, these phenomena are

likely to be as a consequence of prolonged glucose deprivation rather than a direct effect by insulin stimulation.

Considering that critical functions such as regulation of appetite and energy storage are affected when insulin signaling is disrupted in the fly, together with the fact that flies lack a melanocortin system or an AgRP ortholog, it is not surprising that this specific function may have also been conserved in pure NPY neurons in mammals. The appearance during evolution of additional neurotransmitters, like AgRP, now found co-expressed in a set of NPY neurons, probably has added new functional diversity and the ability to fine-tune various neuronal control mechanisms. For example, the action of insulin specifically in AgRP neurons may play a more important role in controlling hepatic glucose production, whereas NPY-only neurons may play a more pronounced role in the regulation of appetite and energy balance. Collectively, our results suggest that insulin signaling in NPY neurons is required for maintaining normal energy homeostasis and that an impaired insulin-NPY signaling pathway may contribute to the development of metabolic diseases.

4. EXPERIMENTAL PROCEDURES

4.1. Animals

All animal care and experiments were approved by the Garvan/St. Vincent's Animal Ethics Committee. $IR^{lox/lox}$, $IR^{lox/lox}$;$NPY^{Cre/+}$, $IR^{lox/lox,tm}$ and $IR^{lox/lox}$;$NPY^{Cre/+,tm}$ mice were generated and genotyped as described in Supplemental Experimental Procedures. Male mice on a mixed C57BL/6–129SvJ background were used for all experiments, except where noted. Mice were housed under a controlled temperature of 22 °C and a 12-h light cycle (lights on from 07:00 to 19:00 h) with *ad libitum* access to water and a standard chow diet (6% calories from fat, 21% calories from protein, 71% calories from carbohydrate, 2.6 kcal/g, Gordon's Specialty Stock Feeds, Australia) or fed a high-fat diet (43% kilojoules from fat, 17% kilojoules from protein, 40% kilojoules from carbohydrate, 4.8 kcal/g, Specialty Feeds, Australia) for 8 weeks starting from 7 to 8 weeks of age.

4.2. Fly studies

Fly stocks were maintained on standard diet and were raised in 25 °C incubator with a 12/12 light/dark cycle. Wild type *w1118* are from Hugo Bellen, *NPF-Gal* was from Ping Shen, *UAS-InR-IR* (#35251) was from the Bloomington Stock Centre. All stocks were backcrossed to wildtype *w1118*. Food intake was measured by CAFÉ assay, which was modified from previous studies [43,44]. Glycogen was determined by measuring the glucose degraded from glycogen using amyloglucosidases. Locomotor activity was determined using the DAM (Drosophila Activity Monitor) system (Trikinetics), which records activity when a fly crosses an infrared beam. The starvation assay was carried with DAM system as described in Supplemental Experimental Procedures.

4.3. Quantitative real-time PCR

Hypothalami were dissected and immediately frozen in liquid N_2, and RNA was extracted using Trizol Reagent (Sigma, St. Louis, MO) and processed for quantitative real-time PCR (Q-PCR) with the Light-Cycler 480 Real-Time PCR system (Roche, Switzerland) as described in the Supplemental Experimental Procedures.

4.4. Metabolic measurements and body composition

Weekly body weight was determined from 4 weeks of age. Food intake was examined in chow- and high fat-fed mice under normal and fasting states as described in Supplemental Experimental Procedures. Whole-body lean and fat masses were determined by DXA (Lunar Piximus II mouse densitometer; GE Healthcare, UK) as previously described [45]. Energy expenditure, RER, and physical activity were assessed using an indirect calorimeter (Oxymax series; Columbus Instruments, Columbus, OH) as described in Supplemental Experimental Procedures.

4.5. Glucose homeostasis assessment and serum assays

Mice were fasted for 4 or 6 h and i.p. administered insulin (0.5 mU/kg body weight, Novo Nordisk Pharmaceuticals, NSW, Australia) or glucose (1 mg/kg body weight, Pharmalab, NSW, Australia). Blood glucose levels were assessed at 0, 15, 30, 60, and 90 min after glucose administration using a Accu-chek® Go glucometer (Roche, Dee Why, Australia). Fed serum was collected and stored for subsequent insulin assay. Serum insulin (Millipore Co, MA, USA) and IGF-1 levels were measured with commercially available ELISA kits (ALPCO Diagnostics, NH, USA) in accordance with the manufacturers' specifications. Hyperinsulinemic-euglycemic clamps were performed on anesthetized mice after 5 h fasting and glucose uptake determined at the end of the clamp after bolus 2-[1-^{14}C]-deoxyglucose administration as described in Supplemental Experimental Procedures.

4.6. Immunohistochemistry

Animals were anesthetized and the brains were perfused with saline and then 4% paraformaldehyde (PFA). Brains were post fixed in 4% PFA, then placed in 30% sucrose overnight and cut at 40 μm on a cryostat. Subsequently, immunohistochemistry was performed using antibodies against phosphorylation Ser473-Akt (Cell Signaling, USA). p-Akt and mCherry expression were visualized in brain sections with a confocal microscope (Olympus, Tokyo, Japan) as described in Supplemental Experimental Procedures.

4.7. *In situ* hybridization study

Coronal brain sections (30 μm) were cut on a cryostat and mounted on slides. Matching sections from the same coronal brain level from different groups of mice were examined together using radiolabeled DNA oligonucleotides complementary to mouse NPY, POMC, and AgRP. Sequence of probes and details of the *in situ* hybridization methodology can be found in Supplemental Experimental Procedures. Slides were visualized and imaged with a light microscope (Leica, Heerbrugg, Switzerland) and quantified using ImageJ64 software (National Institute of Health, USA).

4.8. Intracerebroventricular administration of insulin and analysis of insulin signaling

Adult mice were anesthetized and placed on a Kopf stereotaxic frame (David Kopf Instruments, Tujunga, CA, USA). Insulin (10 mU in 2 μl) was injected into the 3rd ventricle at a rate of 0.1 μl/min using a 10 μl Hamilton syringe attached to Micro4 Micro Syringe Pump Controller (World Precision Instruments Inc., Sarasota, USA). The injection coordinates were (from bregma): 0.0 mm lateral, 0.9 mm posterior, −4.8 ventral [46]. Animals were kept on a heating pad during surgery as described in Supplemental Experimental Procedures.

4.9. Statistical analyses

All data are expressed as mean ± SEM. A two-tailed student's t-test was used to test difference between 2 groups of mice. Differences among groups of mice were assessed by two-way ANOVA or repeated-measures ANOVA. Bonferroni post-hoc and Log-rank tests were performed to identify differences among means. For fly studies, one-way ANOVA with Welch's correction was used. Statistical analyses were assessed using Prism software (GraphPad Software, Inc, LaJolla, CA, USA). Differences were regarded as statistically significant if *$p < 0.05$, **$p < 0.01$.

ACKNOWLEDGEMENTS

This work was supported by the National Health and Medical Research Council (NHMRC) of Australia in the form of a Fellowship to HH and GJC and project grant #1080473 and Diabetes Australia Research Trust project grant to KL.

CONFLICT OF INTEREST

None declared.

APPENDIX A. SUPPLEMENTARY DATA

Supplementary data related to this article can be found at http://dx.doi.org/10.1016/j.molmet.2017.03.013.

REFERENCES

[1] Plum, L., Belgardt, B.F., Bruning, J.C., 2006. Central insulin action in energy and glucose homeostasis. The Journal of Clinical Investigation 116:1761–1766.
[2] Saltiel, A.R., Kahn, C.R., 2001. Insulin signalling and the regulation of glucose and lipid metabolism. Nature 414:799–806.
[3] Air, E.L., Strowski, M.Z., Benoit, S.C., Conarello, S.L., Salituro, G.M., Guan, X.M., et al., 2002. Small molecule insulin mimetics reduce food intake and body weight and prevent development of obesity. Nature Medicine 8:179–183.
[4] Brown, L.M., Clegg, D.J., Benoit, S.C., Woods, S.C., 2006. Intraventricular insulin and leptin reduce food intake and body weight in C57BL/6J mice. Physiology & Behavior 89:687–691.
[5] Hallschmid, M., Benedict, C., Schultes, B., Fehm, H.L., Born, J., Kern, W., 2004. Intranasal insulin reduces body fat in men but not in women. Diabetes 53:3024–3029.
[6] Woods, S.C., Lotter, E.C., McKay, L.D., Porte Jr., D., 1979. Chronic intracerebroventricular infusion of insulin reduces food intake and body weight of baboons. Nature 282:503–505.
[7] Bruning, J.C., Gautam, D., Burks, D.J., Gillette, J., Schubert, M., Orban, P.C., et al., 2000. Role of brain insulin receptor in control of body weight and reproduction. Science 289:2122–2125.
[8] Obici, S., Feng, Z., Karkanias, G., Baskin, D.G., Rossetti, L., 2002. Decreasing hypothalamic insulin receptors causes hyperphagia and insulin resistance in rats. Nature Neuroscience 5:566–572.
[9] Havrankova, J., Roth, J., Brownstein, M., 1978. Insulin receptors are widely distributed in the central nervous system of the rat. Nature 272:827–829.
[10] van Houten, M., Posner, B.I., Kopriwa, B.M., Brawer, J.R., 1979. Insulin-binding sites in the rat brain: in vivo localization to the circumventricular organs by quantitative radioautography. Endocrinology 105:666–673.
[11] Benoit, S.C., Air, E.L., Coolen, L.M., Strauss, R., Jackman, A., Clegg, D.J., et al., 2002. The catabolic action of insulin in the brain is mediated by melanocortins. The Journal of Neuroscience 22:9048–9052.
[12] Schwartz, M.W., Sipols, A.J., Marks, J.L., Sanacora, G., White, J.D., Scheurink, A., et al., 1992. Inhibition of hypothalamic neuropeptide Y gene expression by insulin. Endocrinology 130:3608–3616.
[13] Sipols, A.J., Baskin, D.G., Schwartz, M.W., 1995. Effect of intracerebroventricular insulin infusion on diabetic hyperphagia and hypothalamic neuropeptide gene expression. Diabetes 44:147–151.
[14] Gelling, R.W., Morton, G.J., Morrison, C.D., Niswender, K.D., Myers Jr., M.G., Rhodes, C.J., et al., 2006. Insulin action in the brain contributes to glucose lowering during insulin treatment of diabetes. Cell Metabolism 3:67–73.
[15] Konner, A.C., Bruning, J.C., 2012. Selective insulin and leptin resistance in metabolic disorders. Cell Metabolism 16:144–152.
[16] Loh, K., Herzog, H., Shi, Y.C., 2015. Regulation of energy homeostasis by the NPY system. Trends in Endocrinology and Metabolism 26:125–135.
[17] Luquet, S., Perez, F.A., Hnasko, T.S., Palmiter, R.D., 2005. NPY/AgRP neurons are essential for feeding in adult mice but can be ablated in neonates. Science 310:683–685.
[18] Shi, Y.C., Lau, J., Lin, Z., Zhang, H., Zhai, L., Sperk, G., et al., 2013. Arcuate NPY controls sympathetic output and BAT function via a relay of tyrosine hydroxylase neurons in the PVN. Cell Metabolism 17:236–248.
[19] Wisialowski, T., Parker, R., Preston, E., Sainsbury, A., Kraegen, E., Herzog, H., et al., 2000. Adrenalectomy reduces neuropeptide Y-induced insulin release and NPY receptor expression in the rat ventromedial hypothalamus. The Journal of Clinical Investigation 105:1253–1259.
[20] Ahrén, B., Wierup, N., Sundler, F., 2006. Neuropeptides and the regulation of islet function. Diabetes 55:S98–S107.
[21] Konner, A.C., Janoschek, R., Plum, L., Jordan, S.D., Rother, E., Ma, X., et al., 2007. Insulin action in AgRP-expressing neurons is required for suppression of hepatic glucose production. Cell Metabolism 5:438–449.
[22] Chong, A.C., Vogt, M.C., Hill, A.S., Bruning, J.C., Zeltser, L.M., 2015. Central insulin signaling modulates hypothalamus-pituitary-adrenal axis responsiveness. Molecular Metabolism 4:83–92.
[23] Krashes, M.J., DasGupta, S., Vreede, A., White, B., Armstrong, J.D., Waddell, S., 2009. A neural circuit mechanism integrating motivational state with memory expression in Drosophila. Cell 139:416–427.
[24] Tatar, M., Kopelman, A., Epstein, D., Tu, M.P., Yin, C.M., Garofalo, R.S., 2001. A mutant Drosophila insulin receptor homolog that extends life-span and impairs neuroendocrine function. Science 292:107–110.
[25] Qi, Y., Purtell, L., Fu, M., Lee, N.J., Aepler, J., Zhang, L., et al., 2016. Snord116 is critical in the regulation of food intake and body weight. Scientific Reports 6:18614.
[27] Baldock, P.A., Sainsbury, A., Couzens, M., Enriquez, R.F., Thomas, G.P., Gardiner, E.M., et al., 2002. Hypothalamic Y2 receptors regulate bone formation. The Journal of Clinical Investigation 109:915–921.
[28] Pierroz, D.D., Catzeflis, C., Aebi, A.C., Rivier, J.E., Aubert, M.L., 1996. Chronic administration of neuropeptide Y into the lateral ventricle inhibits both the pituitary-testicular axis and growth hormone and insulin-like growth factor I secretion in intact adult male rats. Endocrinology 137:3–12.
[29] Rettori, V., Milenkovic, L., Riedel, M., McCann, S.M., 1990. Physiological role of neuropeptide Y (NPY) in control of anterior pituitary hormone release in the rat. Endocrinologia Experimentalis 24:37–45.
[30] Lichanska, A.M., Waters, M.J., 2008. How growth hormone controls growth, obesity and sexual dimorphism. Trends in Genetics 24:41–47.
[31] van den Hoek, A.M., van Heijningen, C., Schroder-van der Elst, J.P., Ouwens, D.M., Havekes, L.M., Romijn, J.A., et al., 2008. Intracerebroventricular administration of neuropeptide Y induces hepatic insulin resistance via sympathetic innervation. Diabetes 57:2304–2310.
[32] van den Hoek, A.M., Voshol, P.J., Karnekamp, B.N., Buijs, R.M., Romijn, J.A., Havekes, L.M., et al., 2004. Intracerebroventricular neuropeptide Y infusion precludes inhibition of glucose and VLDL production by insulin. Diabetes 53:2529–2534.
[33] Carvalheira, J.B., Ribeiro, E.B., Araujo, E.P., Guimaraes, R.B., Telles, M.M., Torsoni, M., et al., 2003. Selective impairment of insulin signalling in the hypothalamus of obese Zucker rats. Diabetologia 46:1629–1640.
[34] Hahn, T.M., Breininger, J.F., Baskin, D.G., Schwartz, M.W., 1998. Coexpression of Agrp and NPY in fasting-activated hypothalamic neurons. Nature Neuroscience 1:271–272.
[35] Campbell, J.N., Macosko, E.Z., Fenselau, H., Pers, T.H., Lyubetskaya, A., Tenen, D., et al., 2017. A molecular census of arcuate hypothalamus and median eminence cell types. Nature Neuroscience 20:484–496.
[36] Areias, M.F., Prada, P.O., 2015. Mechanisms of insulin resistance in the amygdala: influences on food intake. Behavioural Brain Research 282:209–217.
[37] Castro, G., MF, C.A., Weissmann, L., Quaresma, P.G., Katashima, C.K., Saad, M.J., et al., 2013 Sep 11. Diet-induced obesity induces endoplasmic reticulum stress and insulin resistance in the amygdala of rats. FEBS Open Bio 3:443–449.

[38] Begg, D.P., Woods, S.C., 2013. The endocrinology of food intake. Nature Reviews. Endocrinology 9:584–597.
[39] Sindelar, D.K., Palmiter, R.D., Woods, S.C., Schwartz, M.W., 2005. Attenuated feeding responses to circadian and palatability cues in mice lacking neuropeptide Y. Peptides 26:2597–2602.
[40] Turner, N., Cooney, G.J., Kraegen, E.W., Bruce, C.R., 2014. Fatty acid metabolism, energy expenditure and insulin resistance in muscle. The Journal of Endocrinology 220:T61–T79.
[41] Steculorum, S.M., Ruud, J., Karakasilioti, I., Backes, H., Engstrom Ruud, L., Timper, K., et al., 2016. AgRP neurons control systemic insulin sensitivity via myostatin expression in brown adipose tissue. Cell 165:125–138.
[42] Sindelar, D.K., Ste Marie, L., Miura, G.I., Palmiter, R.D., McMinn, J.E., Morton, G.J., et al., 2004. Neuropeptide Y is required for hyperphagic feeding in response to neuroglucopenia. Endocrinology 145:3363–3368.
[43] Deshpande, S.A., Carvalho, G.B., Amador, A., Phillips, A.M., Hoxha, S., Lizotte, K.J., et al., 2014. Quantifying Drosophila food intake: comparative analysis of current methodology. Nature Methods 11:535–540.
[44] Ja, W.W., Carvalho, G.B., Mak, E.M., de la Rosa, N.N., Fang, A.Y., Liong, J.C., et al., 2007. Prandiology of Drosophila and the CAFE assay. Proceedings of the National Academy of Sciences of the United States of America 104:8253–8256.
[45] Yulyaningsih, E., Loh, K., Lin, S., Lau, J., Zhang, L., Shi, Y., et al., 2014. Pancreatic polypeptide controls energy homeostasis via Npy6r signaling in the suprachiasmatic nucleus in mice. Cell Metabolism 19:58–72.
[46] Franklin, K.B.J., Paxinos, G., 1997. The mouse brain in stereotaxic coordinates. San Diego: Academic Press.

